Int. J. Heat Mass Transfer. Vol. 13, pp. 1441–1457. Pergamon Press 1970. Printed in Great Britain

CONCENTRATION POLARIZATION IN AN UNSTIRRED BATCH CELL: MEASUREMENTS AND COMPARISON WITH THEORY

M. K. LIU and F. A. WILLIAMS

Department of the Aerospace and Mechanical Engineering Sciences,
University of California, San Diego, La Jolla, California, U.S.A.

(*Received* 15 *May* 1969 *and in revised form* 30 *December* 1969)

Abstract—Experimental and theoretical results are reported for a model that aids in understanding the performance of desalination equipment based on reverse osmosis. The model consists of a cylinder closed by a semipermeable membrane at one end and connected to a pressurization chamber at the other. The one-dimensional, transient flow in the device is governed by a salt diffusion equation which contains a quadratically nonlinear convective term and which is subject to a quadratically nonlinear boundary condition applied at the surface of the membrane. The salt rejection coefficient R for the membrane and the ratio δ of initial osmotic pressure difference to hydrostatic pressure difference across the membrane occur as parameters. Summaries are given of results from extensions of previous theoretical solutions for the time development of salt concentration profiles and for the time dependence of the rate at which water flows through the membrane. Discussions are given of flow-rate measurements and of the use of specially developed electrical conductivity microprobes for measuring pointwise salt concentration histories directly. Experimental results for flow rates and concentration histories, accurate within 5–10 per cent, are presented and compared with theories for three cases, $\delta \ll 1$, $1 - \delta \ll 1$ and intermediate values of δ. Values of R range from 0·8 to 0·99 with $MgSO_4$ solutions at applied pressures below 150 psi. The experimental results support each theory in its proper range of applicability. They reveal the existence of an intermediate range of time inside which none of the theories agree with experiment within 10 per cent.

1. INTRODUCTION

ONE OF the competitive processes for producing fresh water from brine is "reverse osmosis" or "hyperfiltration." Although applications of this process are in a relatively early stage of development, a considerably extensive literature exists on research into the characterization and utilization of the technique. Most of this literature is concerned either with membrane development or with performance of systems involving complex flow channeling. In a small portion of the literature on the subject, a number of theoretical analyses have been published on the behavior of continuous reverse-osmosis flow systems with various simple geometries. The motivation for the theories is to develop a sufficiently detailed understanding of the flow field and of the troublesome phenomenon termed "concentration polarization"—the buildup of excessive amounts of dissolved salt adjacent to the membrane—for engineers to be able to improve performance of desalination systems on the basis of rational design procedures.

Experimental work on flow systems with simple geometrical configurations is desirable as a means for testing the accuracy of the theoretical analyses. In the past, the most direct measurements that could be attempted were observations of the rates at which water and salt flow through the membrane under carefully established brine flow conditions. It is now possible to supplement these observations with more direct, essentially pointwise measurements of salt concentrations on the brine side of the membrane, by using electrical conductivity microprobes, developed by Hendricks. [2] The experimental salt concentration histories so

obtained provide a more stringent test for theoretically calculated concentration fields than do the usual measurements of flow-through rates. The present paper contains the results of measurements made with the new microprobes.

Because of the analogy between two-dimensional steady flow and one-dimensional transient flow, much knowledge of the behavior of continuous reverse osmosis systems can be gleaned by studying the very simple batch distillation process illustrated in Fig. 1. Moreover, this

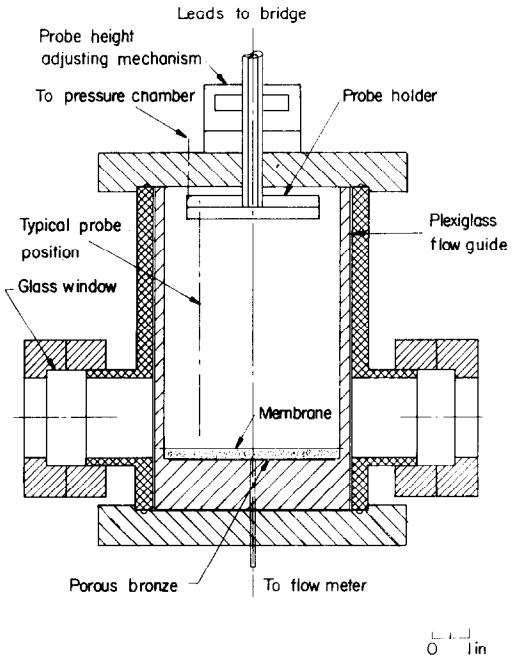

FIG. 1. Desalination cell.

batch process may be of practical interest in itself for certain low-yield production applications and also as a laboratory tool for measuring membrane constants. Nevertheless, very few investigations of unstirred batch cells can be found in the literature. Only a handful of theoretical studies [1, 5, 6, 8] and some experimental results on flow-through rates and salinity on the effluent side [6, 8, 9] have been reported. For many years membrane constants have been obtained from flow-through rates measured in batch cells, but these cells are usually stirred and have geometries and flow fields that are difficult to characterize accurately.

The intention of the present work is to help remedy the deficiency of unstirred batch-cell studies by reporting on improved measurements of flow-through rates and on measurements of salt concentration histories at points within the brine for such systems. The experimental results will be useful in understanding the phenomena and may be compared with theories in an effort to assess their relative accuracies. To facilitate comprehension and comparison with theories, we define the system mathematically in the following section, and in Appendix A we present in a uniform notation a complete summary of currently available theoretical results. Appendix A contains a number of previously unpublished theoretical formulas, which we have derived as extensions to existing theories. Our extensions primarily involve taking into account simultaneously imperfect salt rejection and a nonzero ratio of osmotic to applied pressure. These extensions are needed for comparison with our experimental results.

2. MATHEMATICAL DEFINITION OF FLOW SYSTEM

The volume flow per unit surface area for water passing through the semipermeable membrane is

$$v_w = A(\Delta p - \Delta\pi), \tag{1}$$

where A is the "membrane constant", Δp is the hydrostatic pressure difference across the membrane and $\Delta\pi$ is the difference between the osmotic pressure of the salt solution and that of the effluent. In the present experiment Δp is held constant for time $t \geqslant 0$.

The rejection coefficient R for the membrane is defined in such a way that $1 - R$ is the constant ratio of the effluent salt concentration to the salt concentration in the brine at the upper surface of the membrane, c_w. Then $\Delta\pi$ may be approximated as

$$\Delta\pi = R\pi_0(c_w/c_0), \tag{2}$$

where π_0 is the osmotic pressure of the uniform solution, with salt concentration c_0, contained in the cell at $t = 0$. Equation (2) presumes that the solution is ideal; its accuracy varies from 2 to 20 per cent for the present experiments.

Since mass conservation and incompressibility require that the velocity of the fluid be independent of the distance x normal to the upper surface of the membrane, in a dilute isothermal solution the one-dimensional time-dependent diffusion equation describing the salt concentration field c within the cell is

$$\frac{\partial c}{\partial t} - v_w \frac{\partial c}{\partial x} = D \frac{\partial^2 c}{\partial x^2}, \tag{3}$$

where D is the diffusion coefficient for salt. A balance of diffusive plus convective salt flux across the membrane provides the boundary condition

$$Rv_w c_w = -D(\partial c/\partial x)_w, \tag{4}$$

where the subscript w identifies conditions at $x = 0$. The remaining conditions to which equation (3) is subjected are

$$\begin{aligned} &c \to c_0 \text{ as } x \to \infty \ (t \geqslant 0); \\ &c = c_0 \text{ at } t = 0 \ (x \geqslant 0). \end{aligned} \tag{5}$$

Equations (1)–(5) specify a mathematical problem which possesses a unique solution for $c(x, t)$, the salt concentration field in the unstirred batch cell. This two-parameter, quadratically nonlinear problem can be written in the form

$$\left.\begin{aligned} &\frac{\partial c}{\partial \tau} - (1 - \delta c_w/c_0)\frac{\partial c}{\partial \eta} = \frac{\partial^2 c}{\partial \eta^2}, \\ &(\partial c/\partial \eta)_w = -Rc_w(1 - \delta c_w/c_0) \\ &\qquad\qquad \text{at } \eta = 0, \tau \geqslant 0, \\ &c = c_0 \text{ at } \tau = 0, \eta \geqslant 0 \\ &\qquad\qquad \text{and at } \eta = \infty, \tau \geqslant 0, \end{aligned}\right\} \tag{6}$$

where

$$\delta \equiv R\pi_0/\Delta p, \tag{7}$$

$$\tau \equiv A^2(\Delta p)^2 t/D, \tag{8}$$

$$\eta \equiv A(\Delta p) x/D. \tag{9}$$

Approximate solutions to equation (6), which have been obtained by a variety of techniques, are summarized in Appendix A.

3. EXPERIMENTAL EQUIPMENT

3.1 *Desalination cell*

The cylindrical cell shown in Fig. 1 has stainless steel walls and aluminum end plates. It is approximately 8 in. high and 6 in. dia. and is equipped with two glass windows, located just above the membrane, for viewing purposes. The membrane, backed by filter paper, rests on a circular porous bronze plate which is supported by a lucite plate. Water collection channels, machined in the lucite, lead to an axially positioned stainless steel tube which communicates with the flow-measurements apparatus. A plexiglas flow guide placed above the membrane promotes one-dimensionality.

An electrical conductivity probe holder and probe-height adjustment mechanism were installed in the upper plate of the cell. Provision was made for four probes to remain at different fixed heights above the membrane during an experiment. Electrical leads from the probes pass through the probe holder to a switch which can alternately connect each probe to the AC bridge circuit.

Pressurization was achieved by using a high pressure nitrogen gas cylinder equipped with a pressure regulator, a relief valve and a precision pressure gage.

3.2 *Flow-rate measurement apparatus*

The product water flows through a scaled glass pipette containing a trapped air bubble, as illustrated in Fig. 2. The flow rate is obtained by measuring the travel time of the bubble with a stop watch. The two three-way valves (Fig. 2) are adjusted alternately to keep the bubble in the scaled pipette. The readings of this apparatus have been checked against the rising of a liquid column in a standing pipette and were found to

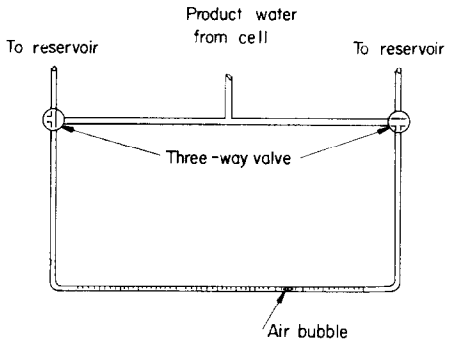

FIG. 2. Sketch of flow-rate measurement device.

be accurate within the error of manipulating the stop watch, perhaps 5 per cent.

3.3 *Measurements of salt concentration*

The use of electrical conductivity microprobes for measuring salt concentration in applications requiring high spatial resolution is becoming increasingly widespread. Such microprobes are now available commercially, (Industrial Science Associates, Inc., Ridgewood, New Jersey) but in the present work probes were constructed in our laboratory following one of the techniques developed by Hendricks [2].

Pure platinum wire of dia. 2·8 mil was inserted into a Pyrex tube of o.d. 35 mil and i.d. 15 mil.

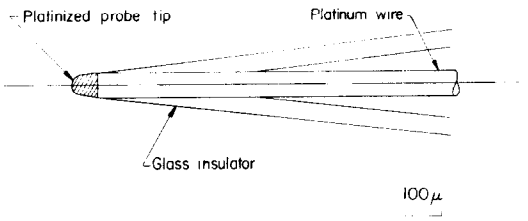

FIG. 3. Conductivity probe.

The center of the tube was then heated and pulled on a Micro-Pipette Puller (Model M1, from Transidyne General Corporation, Ann Arbor, Michigan) to produce a finely tapered glass coating over part of the wire. The protruding end of the wire was then etched in a NaCN solution to achieve the desired shape illustrated in Fig. 3. In later phases of the present experiment the etching and glass-coating steps were interchanged; it was found that glass with an expansion coefficient equal to that of the platinum can be melted onto the etched probe body under a microscope. The tip of the glass-coated etched probe was covered with platinum black by inserting it into a platinizing solution, applying a small negative voltage and monitoring platinum buildup through a microscope. The final probe diameter, ranging from 60 to 75 μ, is sufficiently small to give essentially pointwise measurements in the present application and also leads to quite stable probe readings with acceptable sensitivity.

In measuring solution concentration with the probe, the resistance between the probe and ground (e.g. the wall of the desalination cell) forms one arm of an a.c. bridge which is operated at 25 kc and 300 mV to achieve desired sensitivity and stability. An oscilloscope whose horizontal and vertical deflections are proportional to bridge voltage and error voltage, respectively, was used to balance the bridge. A provision (introduced by Hendricks) for allowing the displayed bridge voltage to be shifted in phase with respect to the error voltage facilitated rapid alternate elimination of capacitive and resistive imbalances.

The operating principle of the probe can be understood as follows. If the probe is approximated as a spherical electrode of radius r immersed in a uniform solution of electrical conductivity σ, then the resistance measured by the bridge is $R_B = R_1 + 1/4\pi r\sigma$, where R_1 is the fixed resistance of the metal and the platinized layer at the probe tip. Since σ is a known function of concentration, a measurement of R_B determines c through this formula. Although the formula gives the correct order of magnitude for any usable probe, since the probe is not exactly spherical a calibration of R_b vs. σ must be made prior to each run by circulating a series of uniform solutions of known concentrations past the probe and recording R_B. The question then arises as to whether the relationship between R_B and σ in the uniform solution

is the same as the relationship between R_B and the local σ in the solution of spatially varying concentration adjacent to the membrane wall. This question has been considered in detail in [10]. The measured R_B reflects the average solution conductivity inside a sphere with diameter of the order of several probe diameters, centered at the probe tip. Within this sphere, solution near the probe tip affects R_B more strongly than solution farther from the probe tip. Theoretical calculations of solutions to the electrical current-flow equation $\nabla.(\sigma\nabla\varphi) = 0$ (where φ is the electrical potential) for representative salt concentration profiles adjacent to an insulating wall, reveal approximately a 10 per cent error in σ when the probe tip is located at a distance $5r$ from the wall [10]. In the present experiments the distance between the probe tip and the wall always exceeded 13 r, and the error in the measured σ caused by both solution nonhomogeneity and the wall is estimated to be less than 3 per cent. An independent indication of the wall effect is obtained when the probe height is adjusted prior to beginning an experiment; the bridge shows a change in probe resistance if the probe is too close to the membrane.

Applications of microelectrodes in electrolyte solutions have often [2, 3, 7, 9] been plagued by loss in sensitivity through "polarization" and by responses that drift in time. It may therefore be worth emphasizing that the probes employed in the present work exhibited excellent sensitifity at 25 kc (revealing fractional changes in c of 1 per cent in a 0·01 M solution) and drifted less than 5 per cent in 24 hr in 0·01 M $MgSO_4$ solutions. The drift is more severe at higher concentrations. The drift limits the accuracy of comparison with asymptotic theories in τ, and the sensitivity limits the accuracy of comparison with theories for small τ or large η, where c differs little from c_0. Probe requirements in batch-cell measurements are appreciably less severe than in continuous-flow measurements, where thin concentration boundary layers necessitate spatial resolution of the order of 10 μ [2].

3.4 *Membrane*

The cellulose acetate membrane used in the present experiment was provided by Gulf General Atomic, Inc., who reported a membrane constant of $A = 1{\cdot}3 \times 10^{-5}$ cm/s atm, and a salt rejection coefficient of $R = 98{\cdot}5$ per cent in 1% NaCl solution at $\Delta p = 800$ psi. In the present work the membrane constant was measured prior to each run by introducing ion-free water into the cell and measuring the flow rate as a function of applied pressure, over the pressure range of the present experiments ($0 < \Delta p \leqslant 150$ psi). The constant slope of v_w vs. Δp yielded $A = 1{\cdot}47 \times 10^{-5}$ cm/s atm, a value which remained unchanged with repeated use of the membrane. Our experimental results discussed below suggest that R depends on Δp, varying from $R = 0{\cdot}87$ at $\Delta p = 30$ psi to $R = 0{\cdot}99$ at $\Delta p = 150$ psi for $MgSO_4$ solutions. It is reasonable to expect rejection to increase with compression.

4. EXPERIMENTAL PROCEDURE

All the tests reported herein were performed with $MgSO_4$ solutions. Magnesium sulfate was selected because it is known to be relatively non-corrosive to metal parts of the cell and because divalent ions generally have high membrane rejection coefficients. The last consideration is particularly important in the present experiment, because rejection is low at low Δp, and the maximum allowable Δp for the present cell is 250 psi. A penalty for using the divalent salt is that the solution deviates from ideality at lower concentrations. Since the theories postulate an osmotic coefficient Φ of unity, the experiments were performed at very dilute concentrations, of the order of 0·01 M, where Φ differs from unity by about 4 per cent.

The laboratory temperature is thermostatically controlled to $20 \pm 1°C$, and the cell and solution are thermally equilibrated with the laboratory before beginning an experiment. The temperature dependence of such quantities as the diffusion coefficient is therefore negligible, and thermally induced flows are not present.

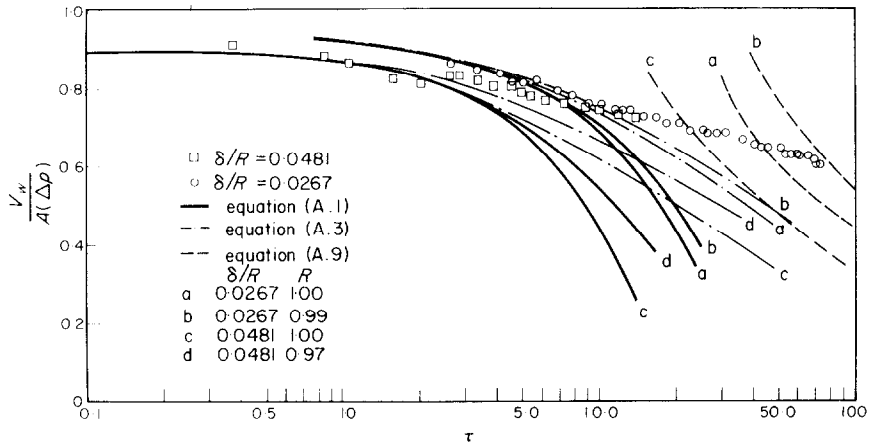

FIG. 4. Time dependence of flow rate for $\delta \ll 1$.

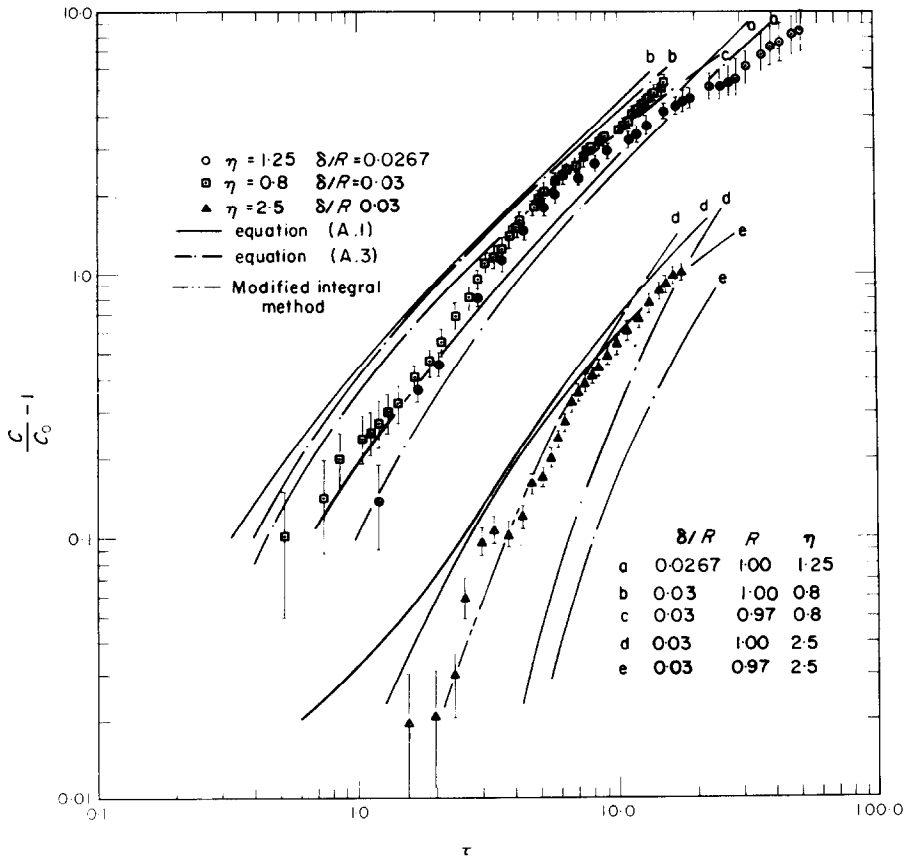

FIG. 5. Concentration histories for $\delta \ll 1$.

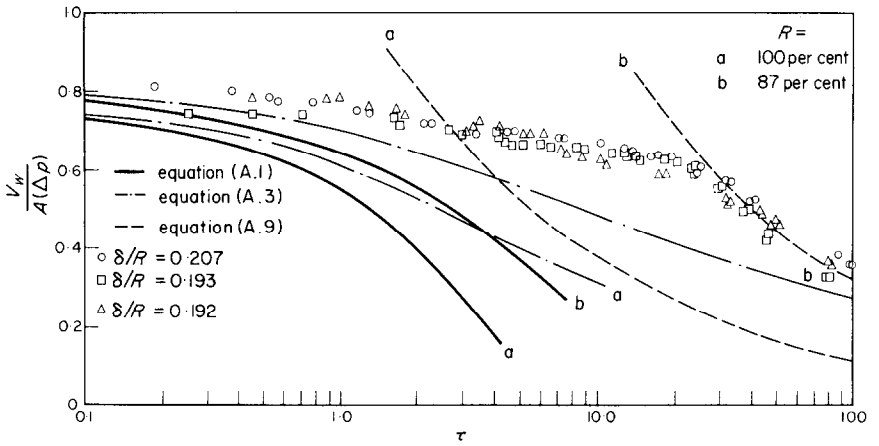

FIG. 6. Time dependence of flow rate for medium values of δ.

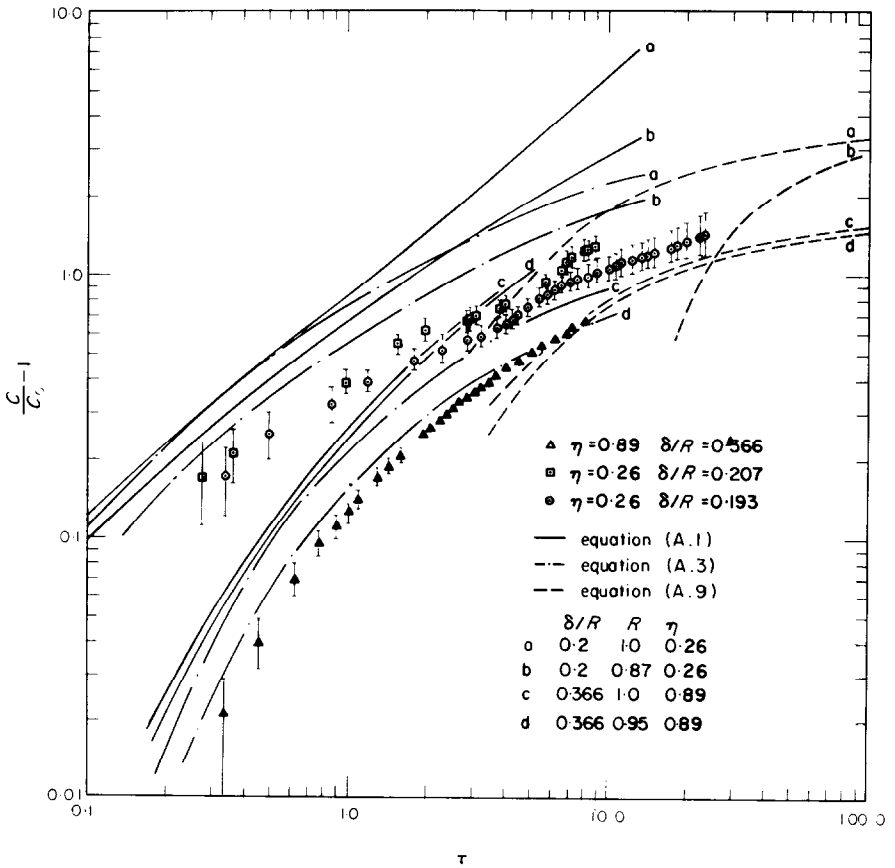

FIG. 7. Concentration histories for medium values of δ.

First the membrane constant is measured, then the probes are calibrated. Calibration is performed with the probes located within the cell a few cm above the membrane. In some cases the calibration procedure is repeated after a run to correct for drift.

After calibration, a uniform solution of desired concentration is circulated into the cell, the probes are positioned near the membrane, and the system is pressurized to begin the run. Concentrations and flow rates are recorded during the run. From 15 to 20 min elapse between stopping the circulation pump and starting the run. In this time major circulation currents die out, but some small residual currents must remain. Probe drift and the occurrence of normal osmosis prevent us from waiting longer for circulation to cease, but persisting circulation velocities in the critical region, the thin concentration layer adjacent to the membrane, can be estimated by simple analysis to be negligibly small. These estimates plus the observation that the experimental results are independent of the way in which the cell is filled indicate that the experiment closely approximates the system defined in Section 2.

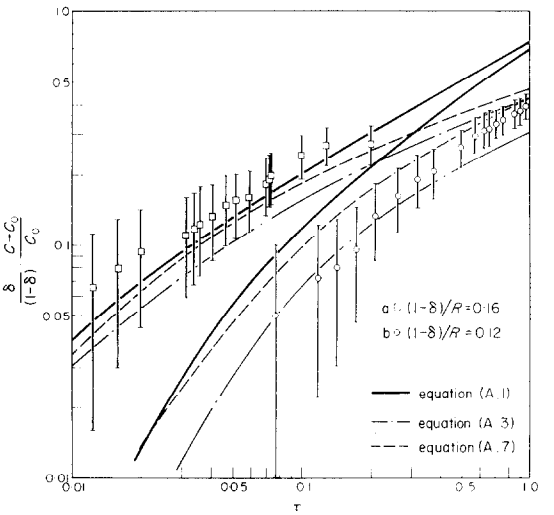

FIG. 9. Concentration histories for $1 - \delta \ll 1$.

In order to test the validity of each theory, experiments were performed for $\delta \ll 1$, for an intermediate value of δ, and for $1 - \delta \ll 1$. Results appear in Figs. 4, 6 and 8 for flow rate and in Figs. 5, 7 and 9 for concentration. The test conditions corresponding to each of these figures are listed in Table 1. The membrane rejects $MgSO_4$ so highly that all experimental

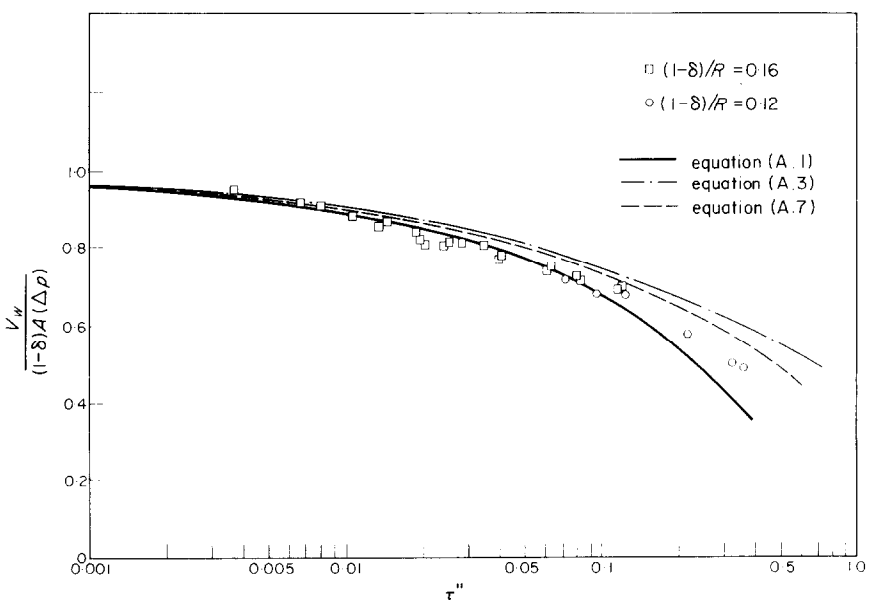

FIG. 8. Time dependence of flow rate for $1 - \delta \ll 1$.

Table 1

Figure	δ/R	Δp (psi)	R (%)	π_0 (psi)	c_0 (M)	x (in)	η
4	0·0267	150	99	4·0	0·00565	—	—
	0·0481	90	97	4·33	0·00615	—	—
5	0·0267	150	99	4·0	0·00565	0·02	1·25
	0·03	97	97	2·94	0·00415	0·02	0·8
	0·03	97	97	2·94	0·00415	0·06	2·5
6	0·193	30·8	87	5·94	0·0084	—	—
	0·192	30	87	6·18	0·00874	—	—
	0·207	32	87	6·19	0·00875	—	—
7	0·207	32	87	6·19	0·00875	0·02	0·26
	0·193	30·8	87	5·94	0·0084	0·02	0·26
	0·366	80·3	95	29·4	0·0415	0·026	0·89
8	1·09	8·3	80	9·04	0·0128	—	—
	1·03	28·7	87	29·6	0·048	—	—
9	1·09	8·3	80	9·04	0·0128	0·02	0·068
	1·03	28·7	87	29·6	0·048	0·02	0·235

conditions appear to fall within the upper left-hand half of Fig. 10. Thus, the experiments do not test equations (A.11) and (A.12). In contrast, the experiments of [6] fall within the lower right-hand half of Fig. 10.

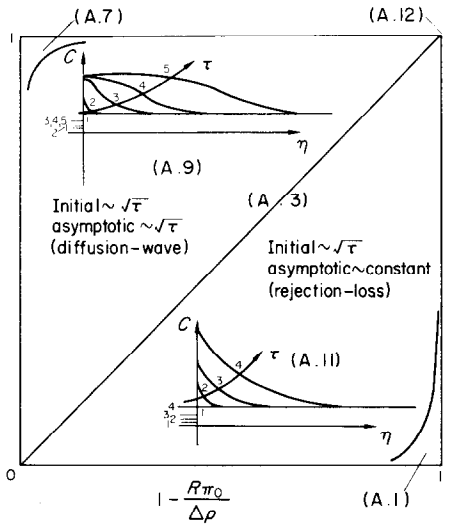

FIG. 10. Illustration of theoretical results.

5. RESULTS AND COMPARISON WITH THEORY

5.1 *The case* $\delta \ll 1$

Figures 4 and 5 illustrate the results for the case $\delta \ll 1$. For the flow rate, Fig. 4 shows that at early time ($\tau < 8$ for $\delta/R = 0{\cdot}0267$ and $\tau < 3$ for $\delta/R = 0{\cdot}0481$) equation (A.1) with $R = 1$ agrees with experiment within about 5 per cent, which is comparable with the experimental inaccuracy of the flow-rate measurement. The flow rate predicted by equation (A.3) (the integral method) with $R = 1$ is almost indistinguishable from that of equation (A.1) (the small-τ theory) at small values of τ and lies closer to the experimental results at larger τ. However, this integral theory departs substantially (>10 per cent) from experiment when $\tau > 20$, and for $\delta/R = 0{\cdot}0267$ the flow rate from the asymptotic theory, equation (A.9), crosses the experimental curve if $R = 1$. This suggests that the membrane is not perfectly impermeable to salt, since the asymptotic curve which is shown for $\delta/R = 0{\cdot}267$ with $R = 0{\cdot}99$ indicates that the experimental points approach an asymptotic theory with R slightly above 0·99. From the curves labeled b for equations (A.1) and (A.3), it can be seen that setting $R = 0{\cdot}99$ improves agreement at smaller τ as well. However, there remains a range of τ, viz. $20 \lesssim \tau \lesssim 60$, over which all theories exhibit noticeable differences from experiment; the maximum difference occurs at $\tau \approx 50$, where the integral method with $R = 0{\cdot}99$ and the asymptotic theory with

$R = 0{\cdot}99$ both differ from experiment by about 25 per cent. Failure of the asymptotic theory in this range is expected since its derivation requires $\tau \gg 1/2\delta = 18{\cdot}55$. Failure of the integral method probably indicates that the concentration profiles are beginning to develop the diffusion-wave structure (illustrated in Fig. 10) which is not described well by the cubic profile assumed in the integral method. Calculations with the modified integral method for $R = 1$ ($\delta/R = 0{\cdot}0267$), not shown on Fig. 4, yield results which coincide approximately with curve b of equation (A.3), thereby suggesting that the modified integral method with $R = 0{\cdot}99$ would produce only slightly improved agreement between theory and experiment.

The concentration history shown in Fig. 5 for $\delta/R = 0{\cdot}0267$ lends further support to these inferences. The bars on the experimental points represent estimated experimental error; inaccuracies are greatest at small τ because of inadequate probe sensitivity and at large τ because of probe drift. The curves labeled a show that both equations (A.1) and (A.3) are in reasonable agreement with experiment, except for $\tau \gtrsim 20$, where the experimental concentrations begin to fall somewhat below the theoretical curves, as expected from Fig. 4. Curves for equations (A.1) and (A.3) with $R = 0{\cdot}99$ and for modified integral method are not shown in Fig. 5 for $\delta/R = 0{\cdot}0267$ because at the value of η for which measurements were taken they differ only slightly from the corresponding curves with $R = 1$.

For the points in Fig. 4 with $\delta/R = 0{\cdot}0481$, and for the points in Fig. 5 with $\delta/R = 0{\cdot}03$, the values $R = 1$ and $R = 0{\cdot}97$ were selected for comparing theory with experiment because 97 per cent appears to be the best estimate of rejection for these runs. Rejection in these cases is lower than rejection for $\delta/R = 0{\cdot}267$ because Δp is less (see Table 1). The dependence of rejection on Δp is discussed later in connection with Fig. 6. Comparison of theory with experiment in Fig. 4 shows that as δ increases, a decrease occurs in the value of τ at which the small-τ and integral-method results depart from experiment.

The two values of η for which data are shown in Fig. 5 with $\delta/R = 0{\cdot}03$ illustrate how the accuracies of the small-τ and integral methods depend on η. At the smaller value of η, there is little difference among the theories, over the range of τ for which data is shown. The small-τ theory with $R = 0{\cdot}97$ (not shown for the smaller η) falls between curves b and c of the integral method, and results from the modified integral method are slightly below those from the integral method. The integral method with $R = 0{\cdot}97$ appears to agree best with experiment, occasional 20 per cent differences in $c/c_0 - 1$ at low concentrations probably being attributable to experimental error. The agreement is not too bad for all theories.

On the other hand, at the larger value of η there are appreciable differences among theoretical results, and the integral method with $R = 0{\cdot}97$ provides the poorest agreement with experiment. The rejection correction improves agreement for the small-τ theory but worsens agreement for the integral method. Although the modified integral method with $R = 1$ agrees very well with experiment, it appears that correcting this method for rejection will lessen agreement. Of the available theories with $R = 0{\cdot}97$, it appears that the small-τ theory is best over this range of τ at the larger η.

It is understandable that the integral method will be poor at large values of η. This method, as well as its modification, possesses a "boundary-layer thickness" $\eta^*(\tau)$ such that $c = c_0$ for $\eta > \eta^*$. Since $\eta^* \to 0$ as $\tau \to 0$, there exists a minimum τ for any given $\eta > 0$ such that $c/c_0 \equiv 1$ when τ is below the minimum. The minimum τ increases as η increases. The minimum τ causes the slopes of the integral-method curves on Fig. 5 to approach infinity as τ approaches the minimum value. On the other hand, the experimental slopes remain finite, and the small-τ theory maintains a finite slope, which causes it to differ greatly from the integral method. Since the integral

method appears to be the best theory for flow rate and for wall concentration (outside the asymptotic range of τ), its principal undesirable feature seems to be its poor prediction of concentration profiles, particularly at large values of η.

Since the small-τ theory agrees reasonably well with the measured salt concentrations for $\tau \lesssim 20$ (Fig. 5) but relatively poorly with the measured flow rates for $\tau \gtrsim 5$ (Fig. 4), one may infer that conclusions concerning the validity of a theory, obtained by comparison with experimental measurements, depend on the types of measurements that are performed. A theory can simultaneously predict good concentration profiles at some distance from the membrane and poor flow-through rates. For a thorough experimental test of all aspects of a theory, flow-rate measurements alone are not sufficient.

5.2 *Intermediate values of* δ

Figure 6 shows flow-rate data from three separate runs for which δ/R differs from 0·2 by less than 4 per cent. Concentration histories at $\eta = 0{\cdot}3$ appear in Fig. 7 for two of these runs. The theoretical curves which were plotted for comparison with this data all have $\delta/R = 0{\cdot}2$, since the difference between this value and each experimental δ/R affects the theoretical results negligibly. It therefore seems reasonable to assume that the differences between the experimental points represent scatter, which is an empirical indication of experimental accuracy. The scatter suggests accuracies of 5–10 per cent in flow rate and perhaps 15 per cent in $c/c_0 - 1$ (i.e. 5–10 per cent in concentration). These accuracies are somewhat poorer than those quoted in Section 3 because they include errors other than instrumental errors (e.g. errors in reproducing the same experimental conditions).

Observations that can be made from Fig. 6 are qualitatively similar to those from Fig. 4. The theoretical curves for $R = 1$ are in very poor agreement with experiment; it is noteworthy that at large τ the data lies far above the asymptotic theory with $R = 1$. Setting $R = 0{\cdot}87$ greatly improves agreement, bringing the asymptotic theory into coincidence with the data for $\tau > 25$. The small-τ theory with $R = 0{\cdot}87$ departs from the data at $\tau \approx 0{\cdot}5$, relatively earlier than the departure in Fig. 4 because δ here is larger. The integral method with $R = 0{\cdot}87$ provides the closest agreement with experiment, although it is in error by 40 per cent at $\tau = 20$. None of the theories agree with the data within 10 per cent when τ lies between 2 and 20. This disagreement is reflected in the fact that the theoretical curves in Fig. 7 fall above the data for $\delta/R = 0{\cdot}2$; the concentration histories in Fig. 7 appear at large τ to be approaching the curve obtained from the asymptotic theory with $R = 0{\cdot}87$.

It is clear from these results that if one is to choose a constant rejection coefficient for $\delta/R = 0{\cdot}2$ which makes the points of agreement between experiment and the various theories entirely comprehensible, then the choice must be $R = 0{\cdot}87$. It is of interest to consider whether this choice makes sense from the viewpoint of membrane properties. If it is assumed that compression increases rejection, then our rejection coefficients consistently exhibit the proper trend in their dependence on Δp (see Table 1). The lower rejection coefficient in Fig. 6 (as compared with Fig. 4) would then be explained by the lower Δp. However, the various theories which have been proposed for membrane properties [4] generally lead to rejection coefficients that vary with $(\Delta p - \Delta\pi)$ rather than Δp. If R is a function of $\Delta p - \Delta\pi$, then it is not exactly constant in our experiments. Thought should therefore be given to comparing our data with theories for which R varies with τ.

No concentration–polarization theories have been worked out with a τ-dependent R. If the dependence of R on $\Delta p - \Delta\pi$ obtained from membrane theories [4] is used in equation (6), then the equation becomes exceedingly nonlinear and should best contain an additional parameter. Development of a proper theoretical analysis would therefore be a complicated task. It appears that if R depends on τ in our experi-

ments, then the τ dependence is slow enough for us to obtain an indication of the degree of agreement between experiment and a theory with a τ-dependent R, by assuming that conditions gradually move from one constant-R to another, with the value of R in each constant-R theory being taken as the value that prevails at the instantaneous value of τ. Adopting this viewpoint and considering as an example the integral-method theory, we find that R would have to decrease from 0·87 at $\tau = 0$ to about 0·7 at $\tau = 20$ and then increase again to about 0·85 at $\tau = 100$, for the integral method to coincide with the data of Fig. 6. The required increase in R at large τ is exceedingly unlikely and is inconsistent with membrane theories [4]. Therefore it seems most reasonable to infer that R is independent of τ in the present tests and that it is proper to compare our results with constant-R theories. Since $\Delta p - \Delta\pi$ typically changes by a factor of two during our runs, we appear to have evidence that in contradiction with the usual membrane theories [4], R depends measurably on Δp but not measurably on $\Delta p - \Delta\pi$.

The data in Fig. 7 with $\delta/R = 0{\cdot}366$ was taken at a higher Δp, corresponding to $R \approx 0{\cdot}95$. The higher value of δ is seen to cause the integral method to be in appreciably better agreement with experiment than the small-τ theory. Calculations (not shown) with the modified integral method for $R = 1$ suggest that the modified integral method with $R = 0{\cdot}95$ would agree quite well with the experimental points. The data appear at large τ to approach tke asymptotic theory with $R = 0{\cdot}95$. These results suggest that as δ increases above 0·3, the flow-rate discrepancy between the integral method and experiment at intermediate values of τ will decrease. Discrepancies due to nonideality of the solution may be important (effects up to 20 per cent) for the comparisons at $\delta/R = 0{\cdot}366$ because of the relatively high concentration (see Table 1 and Fig. 7).

5.3 *The case* $1 - \delta \ll 1$

Figures 8 and 9 show flow rates and concentrations for $1 - \delta \ll 1$. Were R to depend on $\Delta p - \Delta\pi$, it would have to be exceedingly small for these tests—too small to achieve any degree of agreement between theory and experiment. the correlation of R with Δp suggests that $R = 0{\cdot}87$ for $(1 - \delta)/R = 0{\cdot}16$ and that within 10 per cent $R = 0{\cdot}8$ for $(1 - \delta)/R = 0{\cdot}12$ (see Table 1). With these values, generally good agreement of theory with experiment is obtained in Figs. 8 and 9. In Fig. 8 the time variable is τ'' (defined in the appendix) instead of τ; with this variable equation (A.7) (the perturbation theory) predicts a universal curve, while the curves for the integral method and the small-τ theory are not universal but differ negligibly for the two sets of experimental conditions that were chosen. The experimental points in Fig. 8 correlate well with a universal curve and are closest to the results of the perturbation theory. The integral method deviates from experiment at the larger values of τ probably because of the early development of an inflection point in the concentration profile, which is expected at small values of $(1 - \delta)/R$. The small-τ theory begins to deviate from experiment in the anticipated direction for $\tau \gtrsim 0{\cdot}1$; this is especially apparent in Fig. 9. The early failure of the small-τ theory is expected theoretically for $(1 - \delta)/R \ll 1$. Theory also suggests that at later values of τ the convective term in equation (6) will begin to become important, and the perturbation theory will fail; the asymptotic theory should become applicable relatively early, roughly for $\tau \gtrsim 5$. It was not feasible experimentally to run beyond $\tau = 1$ because of the long physical times required at the relatively low values of Δp needed to achieve simultaneously $1 - \delta \ll 1$ and c_0 small enough for the solution to be ideal. The experimental errors in the concentration measurements are substantial in this case because of the sensitivity problems associated with small values of $c/c_0 - 1$.

6. CONCLUSIONS

The primary general conclusion that can be

drawn from this work is that each theory for the concentration field and flow rate appears to agree with experiment within its theoretically anticipated range of validity. It is necessary to take into account a membrane rejection coefficient R, dependent only on the applied hydrostatic pressure Δp, to demonstrate this agreement.

Some of the more specific limitations on the various theories, which have been demonstrated experimentally, are as follows:

The small-τ theory, equation (A.1), is valid for τ less than a maximum value which varies from 10 at $\delta = 0{\cdot}02$ to 0·1 at $\delta = 0{\cdot}9$.

The perturbation theory, equation (A.7), is reasonably accurate for $\tau \lesssim 1$ if $(1 - \delta)/R \lesssim 0{\cdot}2$.

Except at relatively large values of η, the integral method, equation (A.3), agrees well with the small-τ theory and the perturbation theory within the range of τ for which these last two theories agree with experiment. Moreover, the integral method is valid to larger values of τ than the small-τ theory; the integral method is good for $\tau \lesssim 20$ at $\delta = 0{\cdot}02$ and for $\tau \lesssim 1$ at $\delta = 0{\cdot}9$. Furthermore, flow rates obtained from the integral method are sometimes good at large values of τ (80–100 for $\delta \approx 0{\cdot}2$). The modified integral method possesses a slightly greater range of validity than the integral method.

The asymptotic theory is accurate at the largest values of τ investigated experimentally (e.g. for $\tau \approx 80$ at $\delta \approx 0{\cdot}025$ and for $20 \lesssim \tau \lesssim 100$ at $\delta \approx 0{\cdot}2$). The value of τ at which the asymptotic theory becomes valid decreases as δ increases.

There exists an intermediate range of τ within which none of the presently available theories agree with experiment within 10 per cent. This range varies with δ; it is $20 \lesssim \tau \lesssim 60$ at $\delta \approx 0{\cdot}025$ and $2 \lesssim \tau \lesssim 20$ at $\delta \approx 0{\cdot}2$, and it is likely to be largest (one order of magnitude) at intermediate values of δ and to approach zero as δ approaches zero or unity. It would be of interest to attempt to derive new analytical solutions that are applicable in this region.

Experimental work has demonstrated that flow rates through the membrane usually can be measured with 5 per cent accuracy. The electrical conductivity microprobes developed in this work typically can be used to measure pointwise salt concentrations with 5–10 per cent accuracy and reproducibility in an unstirred batch cell. Measurements of salt concentration histories can usefully supplement flow-rate measurements in testing approximate theoretical results on concentration polarization.

ACKNOWLEDGEMENTS

We are indebted to T. J. Hendricks for help with this work. The work was sponsored by the Office of Saline Water under Grant No. 14-001-0001-951.

REFERENCES

1. L. Dresner, Boundary layer build-up in the desalination of salt water by reverse osmosis, ORNL Report 3121 (1963).
2. T. J. Hendricks, Unpublished work, University of California, San Diego (1968).
3. G. Jones and S. M. Christian, The measurement of the conductance of electrolytes VI. Galvanic polarization by alternating current, *J. Am. Chem. Soc.* **57**, 272–280 (1935); G. Jones and D. M. Bollinger, The measurements of the conductance of electrolytes VII. On polarization, *J. Am. Chem. Soc.* **57**, 280–284 (1935).
4. U. Merten, *Desalination by Reverse Osmosis*, pp. 15–35. M.I.T. Press, Cambridge, Mass. (1966).
5. Y. Nakano, C. Tien and W. N. Gill, Nonlinear convective diffusion: A hyperfiltration application, *A.I.Ch.E. Jl* **13**, 1092–1098 (1967).
6. R. J. Raridon, L. Dresner and K. A. Kraus, Hyperfiltration studies V. Salt rejection of membranes by a concentration polarization method, *Desalination* **1**, 210–224 (1966).
7. W. J. Whalen, J. Riley and P. Nair, A microelectrode for measuring intracellular PO_2, *J. Appl. Physiol.* **23**, 798–801 (1967).
8. F. A. Williams, Some properties of the solution to a non-linear diffusion problem relevant to desalination by reverse osmosis, *Siam J. Appl. Math.* **17**, 59–73 (1969).
9. F. A. Williams and T. J. Hendricks, Boundary layer flow problems in desalination by reverse osmosis, OSW Quarterly Report (September 1967).
10. F. A. Williams and T. J. Hendricks, Boundary layer flow problems in desalination by reverse osmosis, OSW Quarterly Report (February 1968).

APPENDIX A

Summary of Theoretical Results

(1) *Dresner* [1, 6] used Laplace transform techniques to obtain a solution to equation (6) for the wall concentration for arbitrary values of $R(0 \leqslant R \leqslant 1)$ under the assumptions that $\delta = 0$ and that the water flux across the membrane is constant. The assumption of constant water flux is valid at sufficiently small values of τ for arbitrary values of $\delta(0 \leqslant \delta \leqslant 1)$. For comparison with the present concentration profile measurements, we have used Laplace transforms to obtain the entire concentration field for arbitrary values of δ and R under the assumption of constant water flux. Our result is

$$\frac{c}{c_0} = 1 + \frac{R}{2(1-R)} e^{-\eta'} \operatorname{erfc}\left(\frac{\eta'}{2\sqrt{\tau'}} - \frac{\sqrt{\tau'}}{2}\right) - \frac{1}{2}\operatorname{erfc}\left(\frac{\eta'}{2\sqrt{\tau'}} + \frac{\sqrt{\tau'}}{2}\right) - \frac{2R-1}{2(1-R)} \exp\left[-R\eta' - R(1-R)\tau'\right] \operatorname{erfc}\left[\frac{\eta'}{2\sqrt{\tau'}} - (2R-1)\frac{\sqrt{\tau'}}{2}\right], \quad (A.1)$$

where

$$\eta' \equiv \eta(1-\delta), \qquad \tau' \equiv \tau(1-\delta)^2. \quad (A.2)$$

The various simplified functional forms for c that are applicable when $R = 1$ or when $\eta = 0$ can be obtained directly from the general formula given in equation (A.1) by formally carrying out mathematical limiting procedures and by using known properties of the complementary error function. The value of τ at which the solution given in equation (A.1) breaks down increases as δ decreases, approaching infinity as δ approaches zero. Hence equation (A.1) should be most useful when $\delta \ll 1$.

For the case $R = 1$, Nakano *et al.* [5] investigated a series expansion in powers of $\sqrt{\tau}$, retaining four terms in the series and presenting results only for c_w and v_w. For $\delta = 0$, over the range $0 \leqslant \tau \leqslant 3$, the result agrees within 0·1 per cent with the limiting form that equation (A.1) assumes when $R = 1$, i.e. the exact solution. With $R = 1$ and $\delta \neq 0$, it is unclear whether the value of τ at which the four-term series breaks down exceeds the value of τ at which equation (A.1) becomes inaccurate.

(2) *Nakano, Tien and Gill* [5] also applied to this problem with $R = 1$ an integral method in which the concentration profile was approximated as a cubic polynomial in η'/a, where $a(\tau')$ is the time-varying thickness of the concentration boundary layer. We have carried out a corresponding analysis for arbitrary value of R. Application of continuity conditions for c and its first two η' derivatives at $\eta' = a$ yields

$$c = \begin{cases} c_0 + (c_w - c_0)(1 - \eta'/a)^3, & \eta' \leqslant a \\ c_0, & \eta' > a \end{cases} \quad (A.3)$$

and the second relation in equation (6) then implies

$$a = (3/R)\left[y/(1+y)\right](1-\alpha y)^{-1}, \quad (A.4)$$

where

$$y \equiv c_w/c_0 - 1, \qquad \alpha \equiv \delta/(1-\delta). \quad (A.5)$$

Substitution of equation (A.3) into the partial differential equation, followed by integration over η', produces a first-order ordinary differential equation in τ', which can be integrated analytically. In terms of the parameter $\gamma \equiv \delta - (1-\delta)(1-R)/R$, the result is

$$\tfrac{4}{3}R^2(1+\alpha)^3\tau' = \frac{1+\alpha}{2\gamma(1-\alpha\gamma)^2} - \frac{\alpha - (1+\alpha)\gamma}{\gamma^2(1-\alpha\gamma)} + \frac{(1-\gamma)^{-1}}{1+\gamma} + \frac{\left[2\alpha - 3(1+\alpha)\gamma\right](1-\gamma) - 2\gamma^2}{2\gamma^2(1-\gamma)} - \frac{2\alpha - (1+2\alpha)\gamma}{(1+\alpha)(1-\gamma)^2}\ln\left(\frac{1+\gamma}{1-\alpha\gamma}\right) + \frac{\alpha^2 - 2\alpha(1+\alpha)\gamma + (1+\alpha)^2\gamma^2}{(1+\alpha)\gamma^3(1-\gamma)^2/(1-2\gamma)}\ln\left[1 + \frac{(1+\alpha)\gamma\gamma}{1-\alpha\gamma}\right], \quad (A.6)$$

which possesses the expected singularity at the origin ($dy/d\tau \sim \tau^{-\frac{1}{2}}$ near $\tau = 0$). Formal limiting procedures applied to equation (A.6) yield reasonable results at such singular points as $R = 1/(1+\alpha)$, which corresponds to the transition condition $R = 1 - \delta$ discussed below.

For the case $R = 1$, Nakano *et al.* [5] improved the results of the simple integral method by treating these results as a zeroth approximation in an iterative technique which they pursued to the first approximation. We have programmed their most accurate result, labelled Y-2 in [5], for evaluating the resulting quadrature numerically on a digital computer. For our experimental conditions the water fluxes and all concentrations except those at large values of η, calculated in this manner, differ at most by 10 per cent from those obtained from the corresponding limiting forms of equations (A.3)–(A.6). In the text we call Y-2 the "modified integral method."

(3) *Williams* [8] employed a perturbation technique to investigate the limiting case in which $1 - \delta \ll R$, $R = 1$. His result can easily be generalized to arbitrary values of R, yielding

$$\frac{c}{c_0} = 1 + \frac{1-\delta}{\delta}\left[\operatorname{erfc}\left(\frac{\eta''}{2\sqrt{\tau''}}\right) - e^{\eta''+\tau''}\operatorname{erfc}\left(\frac{\eta''}{2\sqrt{\tau''}} + \sqrt{\tau''}\right)\right], \quad (A.7)$$

where

$$\eta'' \equiv \eta R, \qquad \tau'' \equiv \tau R^2. \tag{A.8}$$

The theory shows that there exists a range of small η'' and large τ'' for which equation (A.7) is inaccurate when $\delta < 1$.

(4) *Williams* [8] also obtained an asymptotic solution for $\tau \to \infty$ with η fixed, for all values of δ when $R = 1$, by means of an iterative approach. The result can easily be generalized to values of R that satisfy the restriction $R > 1 - \delta$. We obtain

$$\frac{c}{c_0} = \frac{1}{\delta}\left(1 - \sqrt{\frac{\beta}{\tau}}\right)\left\{1 - R\sqrt{(\pi\beta)}\,e^{\beta}\left[\operatorname{erfc}(\sqrt{\beta}) - \operatorname{erfc}\left(\frac{\eta}{2\sqrt{\tau}} + \sqrt{\beta}\right)\right]\right\}, \tag{A.9}$$

where β is defined by the equation

$$e^{\beta}\sqrt{(\pi\beta)}\operatorname{erfc}(\sqrt{\beta}) = (1 - \delta)/R. \tag{A.10}$$

equation (A.9). In [6] the characteristic thickness of the polarization layer asymptotically approaches a constant value, while equation (A.9) indicates that a diffusion "wave" asymptotically spreads away from the membrane producing a characteristic polarization layer thickness which increases without limit in proportion to $\sqrt{\tau}$.

These different asymptotic behaviors result from different operating conditions. This conclusion emerges mathematically from the observations that the derivation of equation (A.9) is restricted to $R > 1 - \delta$ and that as indicated below, a solution possessing the qualities described in [6] can be derived only if $R < 1 - \delta$. Thus, the line $R = 1 - \delta$ in the parameter space separates two regions of very different asymptotic behavior. In terms of the applied pressure and the initial osmotic pressure, this boundary line is $R = \Delta p/(\Delta p + \pi_0)$. The diffusion-wave phenomenon occurs for membranes with good rejection, for high initial osmotic pressure and for low applied pressure. The rejection-loss phenomenon occurs for membranes with poor rejection, for low initial osmotic pressure and for high applied pressure.

Table 2. Approximate theoretical ranges of validity for theoretical results

Equation	τ	η	δ	R
A.1	small, $\tau \ll \tau_m$ ($\tau_m \to \infty$ as $\delta \to 0$)	all	all	all
A.3	all	$\eta' \leqslant a$	all	all
Modified Integral Method	all	$\eta' \leqslant a$	all	1
A.7	$2(1 - \delta)\sqrt{(\tau/\pi)} \ll R\eta + 1$		$1 - \delta \ll R$	all
A.9	large	all	$R > 1 - \delta$	
A.11	large	all	$R < 1 - \delta$	
A.12	large	all	0	1

The restriction on R is needed because the function on the left-hand side of equation (A.10) never exceeds unity.

(5) *Raridon, Dresner and Kraus* [6] discussed an asymptotic solution for $\tau \to \infty$ with η fixed, for all values of R when $\delta = 0$, giving a simple formula for the wall concentration. The physical character of this asymptotic solution is remarkably different from that of the asymptotic solution given in equation (A.9). Reference [6] states that as $\tau \to \infty$ the membrane becomes completely ineffective in removing salt from the feed solution, while equation (A.9) implies that the membrane retains good rejection for all time. In [6] the water flux approaches a finite value as $\tau \to \infty$, while for equation (9) it approaches zero. One can show that for the condition discussed in [6] the slope of the concentration profile is monotonic, while there is an inflection point in

It can be shown from equation (6) that if $R < 1 - \delta$, then as $\tau \to \infty$ with η fixed the time-independent solution

$$\frac{c}{c_0} = 1 + \frac{R}{1 - R}\exp\left[-\left(\frac{1 - \delta - R}{1 - R}\right)\eta\right] \tag{A.11}$$

is approached exponentially in τ. The restriction on R is needed to assure that $c \to c_0$ as $\eta \to \infty$.

For the case $R = 1$, $\delta = 0$, the asymptotic solution to equation (6) is

$$\frac{c}{c_0} = 1 + (\tau - \eta + b)\,e^{-\eta}, \tag{A.12}$$

where b is a constant whose value cannot be determined by considering only the asymptotic range. To solve equation

(6) asymptotically in τ for other values of δ along the transition line $R = 1 - \delta$ is an interesting unsolved problem.

Table 2 summarizes the theoretical ranges of validity for the existing solutions. Figure 10 illustrates these results pictorially in the parameter space. The equation numbers placed on Fig. 10 identify the (R, δ) region in which each equation is most useful. Equations (A.1), (A.3) and (A.7) can be used for nearly all η and τ in their indicated regions, while equations (A.9), (A.11) and (A.12) are asymptotic in τ. Insets illustrate histories of salt concentration profiles and of effluent salt concentrations, on each side of the transition line; the number one identifies the initial profile and the highest numbers the assymptotic profile. Evaluation of the solutions at $\eta = 0$ followed by substitution into equations (1) and (2) gives the membrane flux v_w.

POLARISATION DE CONCENTRATION DANS UNE CUVE SANS AGITATION: MESURES ET COMPARISON AVEC LA THÉORIE

Résumé—Des résultats expérimentaux et théoretiques sont décrits pour un modèle servant à la compréhension de l'action d'un équipement de désalinisation basé sur l'osmose inverse. Le modèle consiste en un cylindre fermé à une extrémité par une membrane semiperméable et relié à l'autre extrémité à une chambre de pressurisation. L'écoulement transitoire unidimensionnel dans l'appareil est régi par une équation de la diffusion du sel qui contient un terme convectif non-linéaire quadratique et qui est soumis à une condition à la limite non-linéaire quadratique appliquée à la surface de la membrane. Le coefficient de rejet du sel R pour la membrane et le rapport de la différence initiale de pression osmotique à la différence de pression hydrostatique de part et d'autre de la membrane se présentent comme paramètres.

On donne les résumés des résultats des extensions des solutions théoriques antérieures pour le développement temporel des profils de concentration en sel et pour la dépendance temporelle de la vitesse avec laquelle l'eau s'écoule à travers la membrane. On donne les discussions des mesures du débit et de l'emploi de microsondes de conductivité électrique fabriquées spécialement pour mesurer directement l'évolution des concentrations locales en sel. Les résultats expérimentaux pour les évolutions des débits et des concentrations, avec une précision allant de 5 à 10 pour cent, sont présentés et comparés avec les théories pour trois cas, $\delta \ll 1$, $1 - \delta \ll 1$, et des valeurs intermédiares de δ. Les valeurs de R variaient de 0,8 à 0.99 avec des solutions de $MgSO_4$ à des pressions appliquées inférieures à 10,33 bars. Les résultats expérimentaux confirment chaque théorie dans son domaine propre d'applicabilité. Ils révèlent l'existence d'un domaine intermédiaire de temps à l'intérieur duquel aucune des théories n'est d'accord avec l'expérience à 10 pour cent près.

KONZENTRATIONSPOLARISATION IN EINER NICHT BEWEGTEN, OSMOTISCHEN ZELLE: MESSUNGEN UND VERGLEICH MIT DER THEORIE

Zusammenfassung—Es wird über experimentelle und theoretische Ergebnisse von Untersuchungen an einem Modell berichtet, das die Funktionsweise von Entsalzungsanlagen, die auf umgekehrter Osmose beruhen, verstehen hilft. Das Modell besteht aus einem Zylinder, der auf der einen Seite von einer halbdurchlässigen Wand abgeschlossen und auf der anderen mit einer Druckerzeugungskammer verbunden ist. Die eindimensionale, instationäre Strömung in der Apparatur wird durch die Gleichung bestimmt, nach der die Salzdiffusion abläuft. Diese Gleichung enthält einen quadratischen, nichtlinearen, konvektiven Term und ist die Ursache für eine quadratische, nichtlineare Randbedingung an der Oberfläche der Membran. Der Koeffizient R für die Membran, der sich auf das nicht durchdiffundierende Salz bezieht und das Verhältnis von anfänglicher osmotischer Druckdifferenz zu hydrostatischer Druckdifferenz an der Membran erscheinen als Parameter. Von den Ergebnissen erweiterter früherer theoretischer Lösungen für die zeitliche Entwicklung der Salzkonzentrationsprofile und für die Zeitabhängigkeit der Konzentration, bei der Wasser durch die Membran fliesst, werden Zusammenfassungen angegeben. Die Messungen der Durchflussmenge werden diskutiert, sowie der Gebrauch speziell entwickelter, die elektrische Leitfähigkeit messender Mikrosonden, um punktweise die Änderung der Salzkonzentration direkt zu messen. Versuchsergebnisse für Durchflussmessungen und Konzentrationsänderungen werden mit einer Genauigkeit von 5 bis 10 Prozent angegeben und mit Theorien für 3 Fälle, nämlich δ und für Zwischenwerte von δ verglichen. Die Werte von R liegen zwischen 0,8 und 0,99 bei $MgSO_4$-Lösungen bei Drücken unter 10 bar. Die experimentellen Ergebnisse bestätigen jede Theorie in ihrem speziellen Anwendungsbereich. Sie zeigen, dass es zeitlich einen Zwischenbereich gibt, innerhalb dessen keine der Theorien mit den Versuchen innerhalb 10 Prozent übereinstimmt.

КОНЦЕНТРАЦИОННАЯ ПОЛЯРИЗАЦИЯ В РАБОТАЮЩЕЙ БЕЗ ПЕРЕМЕШИВАНИЯ ДОЗИРУЮЩЕЙ ЯЧЕЙКЕ. ИЗМЕРЕНИЯ И СРАВНЕНИЯ С ТЕОРИЕЙ

Аннотация—Приводятся экспериментальные и теоретические данные для модели, помогающей понять действие устройства для обессоливания на основе обратного осмосиса. Модель состоит из цилиндра, закрытого с одной стороны полупроницаемой мембраной, а с другой соединяющимся с камерой герметизации. Одномерное неустановившееся течение в устройстве описывается уравнением диффузии соли, содержащем квадратично-нелинейный конвективный член и имеющим квадратично нелинейное граничное условие на поверхности мембраны. Коэффициент выделения соли R для мембраны и отношение разности осмотического давления к разности гидростатического давления на мембране принимаются за параметры. Обобщаются результаты предыдущих теоретических решений для временной зависимости профилей концентрации соли и временной зависимости расхода воды через мембрану. Обсуждаются результаты измерений расхода и использование специального созданных электрокондуктивных микрозондов для непосредственного измерения временной зависимости локальной концентрации соли. Приводятся экспериментальные результаты измерения расходов и концентрации с точностью от 5 до 10%, которые сравниваются с теоретическими результатами, при средних числах R. Значения для раствора $MgSO_4$ колебались от 0,8 до 0,99 при давлениях ниже 1,50 псиа. Экспериментальные значения согласуются с теоретическими.